Ion-Induced Surface Evolution in the Linear Instability Regime: Continuum Theory and Kinetic Monte Carlo Simulations

Eric Chason* and Wai Lun Chan

Division of Engineering, Brown University
Providence RI 02912, USA

Abstract

Low energy ion sputtering produces spontaneous pattern formation on many surfaces. A continuum theory that balances the processes of roughening by sputter removal of atoms and smoothing by surface diffusion of defects explains many features of the early stages of pattern formation. The sputtering is based on a mechanism proposed by Sigmund (1969, 1973) which couples the rate of atom removal to the local surface morphology. Results of kinetic Monte Carlo simulations of surface evolution using the Sigmund mechanism for sputtering are found to agree quantitatively with the predictions of the continuum theory in the linear regime. This suggests that the continuum theory correctly accounts for many of the essential physical mechanisms that lead to the initial formation of the ion-induced pattern.

Contents

* E-mail: eric_chason@brown.edu

1. Introduction

Bombardment by low energy ions (ion sputtering) is a real workhorse when it comes to modifying and characterizing thin films and surfaces. The virtue of low energy ions is that they are able to remove material from the surface without creating so much damage that they destroy the structures that are of interest. Therefore, ion sputtering is frequently used to prepare atomically clean surfaces and to create thin samples for transmission electron microscopy. Analyzing the sputtered surface or the atoms that are sputtered away is used to profile the depth distribution of atoms in thin layers. More recently, focused ion beams (FIB) have enabled nanoscale regions of the sample to be removed selectively for analysis or to create unique structures.

Although the damage by the ion beam is confined mostly to the near surface region, it has been noted by many (Bradley and Harper, 1988; Carter, 2001; Makeev et al., 2002; Valbusa et al., 2002) that prolonged sputtering can lead to the development of pronounced patterns on the surface (sputter ripples). The type of pattern depends on the ion beam, the material being sputtered, and the processing conditions so that arrays of one-dimensional ripples (Mayer et al., 1994; Chason et al., 1994; Carter and Vishnyakov, 1996; Rusponi et al., 1998; Erlebacher et al., 1999; Habenicht, 2001; Umbach et al., 2001), two-dimensional mounds and pits (Ritter et al., 1996; Ernst, 1997; Murty et al., 1998b; Costantini et al., 2001; Michely et al., 2001; Kalff et al., 2001; Malis et al., 2002) and even quantum dot-like structures (Facsko et al., 1999; Gago et al., 2001; Frost et al., 2004) have been observed under different conditions. The wavelength of these patterns ranges from the micron range down to nanometers. From the materials analysis point of view, the excess roughness created by these patterns can degrade the depth resolution (Stevie et al., 1988; Cirlin, 1992; Wittmaack, 1998) and there is interest in understanding their origin in order to control or eliminate them. On the other hand, because ion-induced patterns form spontaneously without needing

any external templates or beam modulation, they are also interesting as a way of inexpensively producing nanoscale structures by means of self-organization. Moreover, the patterning behavior can be used to study the ion-surface interaction and the resulting ion-induced defect kinetics on the surface.

Understanding how sputter ripples form has been the subject of significant analysis over the past twenty-odd years. The fact that the sputter ripples form spontaneously indicates that they originate from the interaction between different processes occurring on the surface during ion bombardment. In the early stages, the behavior can be modeled using a simple linear theory of morphology evolution. As described below, the heart of this model is a sputtering theory developed by Sigmund in which the sputter yield is dependent on the local surface curvature. The overall surface evolution is described analytically in terms of a dynamic balance between roughening by the sputtering process and smoothing by diffusion of point defects (adatoms and surface vacancies) on the surface. As pointed out by Bradley and Harper (BH) (1988), the appearance of a characteristic wavelength can be explained by the mechanism of a linear instability where the competition between different surface processes results in the selection of a preferred range of spatial frequencies that grow faster than any others on the surface.

The goal of this article is to describe the physical mechanisms that determine the evolution of the sputter ripples in the early stage. To explore the validity of this analytical approach, we compare the continuum predictions with recent results of kinetic Monte Carlo (KMC) simulations. The KMC simulations use the Sigmund mechanism to model the sputtering process coupled with diffusion of defects using a solid-on-solid (Chason and Dodson, 1991) model of atomic hopping. Unlike experiments, in the KMC simulations we are able to completely specify all the important parameters for the ion beam and the surface diffusion. The resulting surface morphology enables us to monitor how the surface evolves under the simultaneous action of the sputtering and surface diffusivity for direct comparison with the continuum theory. In addition, the KMC simulations enable us to quantify the surface defect concentrations on the surface during the simulated sputtering process which is not possible in experiments.

2. Continuum Theory of Sputter Ripple Formation

In this section, we discuss different physical mechanisms that operate during low energy ion bombardment to control the evolution of the surface morphology. We use continuum approximations of these mechanisms to derive an analytical expression for the evolution of the surface height $[h(x, y)]$ at different positions x and y on the surface. This treatment follows the approach originally used by

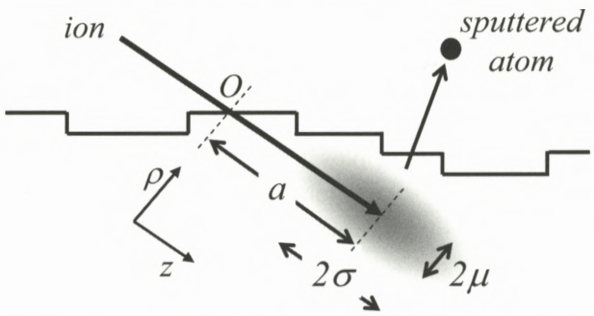

Figure 1. Schematic of Sigmund mechanism for sputtering of atom. The energy deposited by the ion per unit volume is approximated by a Gaussian form that creates elliptical contours around the stopping point. The sputter yield from each surface site is taken to be proportional to the energy deposited there.

Bradley and Harper (1988) to explain the origin of ripple formation in terms of a linear instability mechanism.

2.1. Sigmund Mechanism for Sputtering

The Sigmund theory is an approximation that makes it possible to calculate where an incoming ion will cause an atom to be sputtered from on the surface. In the actual process of sputtering, the energetic ion gives up its kinetic energy in a series of atomic collisions (called the binary collision approximation or BCA). Monte Carlo programs such as SRIM (Ziegler and Biersack, 2000) that are based on the BCA can calculate the details of a series of collisions for an incident ion trajectory. However, because each trajectory contains only a few collisions and is very sensitive to the exact impact parameter, it is not possible to use the BCA approach in an analytical formulation. This difficulty is avoided in the Sigmund theory, where the energy deposited per unit volume averaged over a large number of incident ion trajectories is approximated by a smooth form in which the contours of constant energy deposition form ellipsoids around the center of the distribution (Sigmund 1969, 1973). Therefore, even though each individual trajectory is difficult to predict, the behavior averaged over a large number of incident ions may be treated analytically.

The energy distribution derived by Sigmund is shown schematically in Figure 1. In this figure, the ion enters the surface at the point O and the center of the distribution is at a distance a along the initial ion trajectory. Using coordinates where z is the distance from O along the ion trajectory and ρ is the distance

normal to the trajectory, the energy per unit volume deposited by collisions at each point in the material is described by

$$E(\rho, z) = \varepsilon_0 \exp\left\{-\left[\frac{(z-a)^2}{2\sigma^2} + \frac{\rho^2}{2\mu^2}\right]\right\}, \tag{1}$$

where ε_0 is a normalization factor and the parameters σ and μ describe the width of the energy deposition profile in the directions parallel and perpendicular to the initial trajectory. The amount of material sputtered from each site on the surface is taken to be proportional to the energy deposited at that site, as calculated from Equation (1). The sputter yield, Y, is proportional to the total amount of energy deposited at the surface.

2.2. Sputter Roughening of Surface

Bradley and Harper (1988) used the Sigmund theory to calculate the evolution of the surface topography by integrating the erosion rate calculated from Equation (1) over the entire surface. For topographies in which the radius of curvature on the surface remains large compared to the ion's range a, the erosion rate at each point x and y on the surface can be approximated by the form:

$$\frac{\partial h}{\partial t} = -v_0(\theta) + \Gamma\frac{\partial h}{\partial x} + v_x\frac{\partial^2 h}{\partial x^2} + v_y\frac{\partial^2 h}{\partial y^2}. \tag{2}$$

In this equation, x is oriented parallel to the direction of the ion beam projected onto the surface, i.e., in the same direction as z in Figure 1 projected along the surface and y is in the orthogonal direction on the surface. v_0 is the average rate of erosion of the surface and depends on the angle of incidence, θ, relative to the surface normal Γ accounts for the variation of the sputter yield with the slope of the surface and is equal to $\partial v_0/\partial\theta$. v_x and v_y relate the sputter yield locally to the surface curvature with values that depend on the ion parameters (a, Y, σ, μ) and the angle of incidence; a detailed calculation of v_x and v_y is provided in Makeev et al. (2002). The dependence of the sputter rate on the local curvature means that for a surface with a rough topography the peaks on the surface will sputter slowly and the valleys will sputter quickly. Therefore, in the absence of all other effects, the Sigmund mechanism will make a rough surface become even rougher due to sputtering.

2.3. Surface Diffusion

Surface diffusion will act to smoothen a rough surface by transport of material from regions of high surface energy to regions of low surface energy (as shown

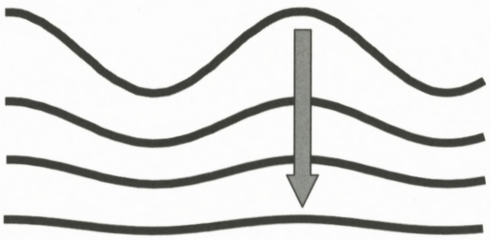

Figure 2. Surface diffusion is modeled using the classical theory of Mullins (1959) and Herring (1950). Surface defects diffuse to decrease the amplitude of modulations on the surface.

schematically in Figure 2). The analytical form for this was described by Mullins (1959) and Herring (1950) and given by:

$$\frac{\partial h}{\partial t} = -B\nabla^4 h, \tag{3a}$$

where

$$B = \frac{\gamma D_s C}{n^2 k_B T}, \tag{3b}$$

and γ is the surface energy, D_s is the diffusivity of a mobile surface defect, C is the concentration of mobile defects on the surface (number per unit area) and n is the number of atoms per unit volume. We define D_s and C in terms of mobile defects (rather than simply adatoms) because surface transport may occur by diffusion of adatoms or surface vacancies when ion bombardment is used. Note that this model for the surface diffusivity does not take into account effects of surface crystallinity and therefore is strictly only appropriate for amorphous surfaces or crystalline surface above the roughening transition. The complications that this entails have been discussed elsewhere (Jeong and Williams, 1999; Israeli and Kandel, 2000; Erlebacher et al., 2000; Pedemonte et al., 2003; Shenoy et al. 2003, 2004; Chan et al., 2004b; Margetis et al., 2004), however we will use this simple linear theory in this work.

2.4. Ion-Induced Smoothing and Higher Order Effects

Makeev and co-workers (Makeev and Barabasi, 1997; Makeev et al., 2002) carried out the calculation of the surface evolution to higher order and recognized that there are other terms that are linear in the surface height besides those included by Bradley and Harper. The effect of this is to add additional terms to Equation (2) of the form:

$$-B_{I,x}\frac{\partial^4 h}{\partial x^4} - B_{I,xy}\frac{\partial^4 h}{\partial x^2 \partial x^2} - B_{I,y}\frac{\partial^4 h}{\partial y^4}. \tag{4}$$

These terms have functional forms that are similar to the diffusional smoothing in Equation (3), i.e., they depend on the fourth derivative of the height and they tend to make the surface smoother. However, these terms derive directly from the interaction of the ion with the surface and have no relation to surface diffusion.

Higher order terms of the form $\partial^3 h/\partial x^3$ and $\partial^3 h/\partial x \partial y^2$ are also present in the linear continuum equation (Makeev et al., 2002). Similar to the effect of the Γ term, these terms affect the propagation of the ripples along the ion beam direction and account for dispersion in the ripple velocity with respect to the wavevector. These effects are observed in our simulation (Chason et al., 2006) but are not discussed further here. Other non-linear terms can be added to these equations to account for long-time behavior (Makeev et al., 2002). However, since the purpose of this work is comparing the continuum theory with KMC simulations, we limit the discussion to the early linear regime of pattern formation where the KMC model is expected to be most valid.

2.5. Ehrlich–Schwoebel Barriers to Interlayer Transport

On metal surfaces, measurements of pattern formation during ion bombardment may depend on the crystallography of the surface and not just the direction of the ion beam. It is suggested (Rusponi et al., 1998; Costantini et al., 2001; Valbusa et al., 2002) that the presence of Ehrlich–Schwoebel barriers that modify interlayer transport can modify the roughening process in a way similar to the mechanism proposed by Villain (1991) and Politi and Villain (1996). Although this effect is not linear, they proposed that in the early stages the roughening behavior could be approximated by a form in which the roughening depends on the local curvature with coefficients S_x and S_y that depend on the barriers to interlayer transport.

In contrast with the BH mechanism, the parameters S_x and S_y depend on temperature while the BH roughening terms (v_x, v_y) only depend on the ion beam parameters. Since the curvature dependence is similar to the BH mechanism, these terms can compete directly with the BH roughening terms. Under certain sputtering conditions, these effects can dominate to produce a different class of surface morphology. In this paper, however, we will only concentrate on regimes in which the BH mechanism is dominant so that roughening induced by Ehrlich–Schwoebel barrier will be neglected. Experimentally, these conditions are fulfilled when the surface is sputtered at a relatively high temperature and flux (Chan et al., 2004a), when the surface has a low Schwoebel barrier (Chason et al., 1994; Erlebacher et al., 1999; Brown and Erlebacher, 2005) or when the surface becomes amorphous (Mayer et al., 1994; Carter and Vishnyakov, 1996; Facsko et al., 1999; Umbach et al., 2001; Habenicht, 2001; Gago et al., 2001; Frost et al., 2004).

2.6. Surface Evolution in the Linear Regime

These mechanisms can be put together to predict the evolution of the surface morphology. Combining Equations (2)–(4), in the linear regime (i.e., the early stages of pattern formation), the continuum equation is written as:

$$\begin{aligned}\frac{\partial h}{\partial t} &= -v_0(\theta) + \Gamma\frac{\partial h}{\partial x} + v_x\frac{\partial^2 h}{\partial x^2} + v_y\frac{\partial^2 h}{\partial y^2} + S_x\frac{\partial^2 h}{\partial x^2} + S_y\frac{\partial^2 h}{\partial y^2} \\ &\quad - B\nabla^4 h - B_{I,x}\frac{\partial^4 h}{\partial x^4} - B_{I,xy}\frac{\partial^4 h}{\partial x^2 \partial x^2} - B_{I,y}\frac{\partial^4 h}{\partial y^4}\,. \end{aligned} \tag{5}$$

This equation can be Fourier transformed so that the amplitude of individual Fourier components on the surface can be calculated. The amplitude of each Fourier component at time t is given by:

$$h_k(t) = h_k(0)\,\mathrm{e}^{r(k_x,k_y)t}\,\mathrm{e}^{ik_x(x+\Gamma t)}, \tag{6a}$$

where $h_k(0)$ is the value of the Fourier coefficient initially and

$$\begin{aligned} r(k_x, k_y) &= -v_x(f)k_x^2 - v_y(f)k_y^2 - S_x(f,T)k_x^2 - S_y(f,T)k_y^2 \\ &\quad - B(f,T)(k_x^2 + k_x^2)^2 - B_{I,x}(f)k_x^4 \\ &\quad - B_{I,xy}(f)k_x^2k_y^2 - B_{I,y}(f)k_y^4\,. \end{aligned} \tag{6b}$$

We call $r(k_x, k_y)$ the amplification factor because it determines the rate at which the amplitude grows or decays. The parameters that determine $r(k_x, k_y)$ have been explained above. The dependence of each parameter on the flux, f, and the temperature, T, has been written explicitly to indicate how f and T impact the growth rate of the ripples.

For positive values of r, the amplitude will increase while for negative values it will decrease. The evolution of the surface morphology is therefore completely determined (in this model, at least) by the value of the amplification factor, r. For a range of parameters, the dependence of r on the magnitude of k has a form that can be represented schematically as shown in Figure 3. Under these conditions, there is a range of k values for which the amplification factor is positive and other values for which it is negative. The amplification factor has a maximum value of r^* which occurs at the wavevector k^*. As a function of time, the amplitude of the Fourier coefficient with wavevector k^* will grow faster than all others and the surface will develop a characteristic periodicity at this spatial frequency.

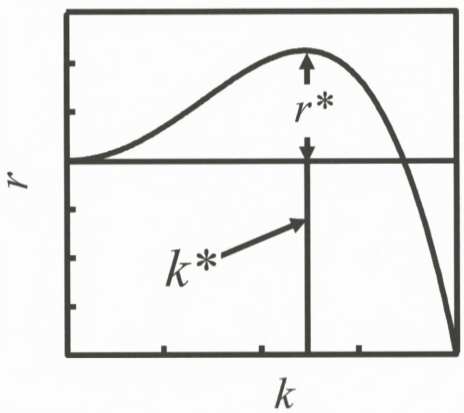

Figure 3. Schematic representation of the amplification rate r as a function of the wavevector k. The amplification factor is maximum (r^*) at the fastest growing wavevector (k^*).

From a linear stability analysis of $r(k_x, k_y)$, we can determine how the wavelength and growth rate of the pattern depend on the parameters of the model:

$$r^* = \frac{v_{\max}^2}{4(B + B_{I,\max})}, \tag{7a}$$

$$k^* = \left(\frac{v_{\max}}{2(B + B_{I,\max})}\right)^{1/2} \tag{7b}$$

The subscript "max" refers to the value $|v_x|$ or $|v_y|$ which has the greater magnitude, i.e., the one that will grow faster on the surface. The wavevector of the pattern will align along the direction corresponding to the larger of these parameters.

From these equations, we have a prediction of how the pattern will evolve based on the parameters of the continuum model. In the following section, we will compare these predictions with results of our KMC simulation to determine how well the instability model compares with an atomistic sputtering picture based on the Sigmund model. Note that in this analysis we have set the value of S_x and S_y equal to zero so that we are ignoring the effect of the Schwoebel barrier. Also note that we are only considering a linear model for the pattern formation here. Non-linear terms are certainly expected to become important as the amplitude of the ripples increases. The comparison with the KMC simulations is therefore only relevant to the early stages of the pattern formation. However, the direct comparison of the model with the simulations is useful even if it is only over a limited range of ripple amplitude.

3. Kinetic Monte Carlo Simulations

The approach to pattern formation described above is based on developing a rate equation for the evolution of the surface height using continuum models for the sputter removal and surface transport. An alternative approach, discussed here, is to develop kinetic Monte Carlo (KMC) computer simulations in which atomistic processes are modeled by transitions on a surface following rules designed to mimic kinetic processes such as diffusion and sputtering. The surface morphology that develops from this approach is the result of the interaction of many independent events that are analogous to the motion of individual atoms and vacancies on the sputtered surface. By comparing the surface morphology evolution between the simulations and the continuum theory, we can directly determine if the continuum theory is a valid approximation for the collective action of the numerous atomic-level events controlling the surface evolution. Furthermore, because we can monitor all the atomic level processes in the KMC simulation, we can also study the defect kinetics that underlie the ion-induced pattern formation.

Previously, simulations have been performed that use the Sigmund mechanism for sputtering but these did not use the same approach as this work for surface transport. In these works, either a simplified relaxation process or a process based on a Monte Carlo (MC) algorithm to determine the equilibrium state was employed (Cuerno et al., 1995; Koponen et al., 1997; Hartmann et al., 2002; Stepanova and Dew 2004; Yewande et al., 2005) so that they did not model the non-equlibrium surface dynamics. On the other hand, previous simulations that do employ diffusion processes with thermally activated hopping rates did not use the Sigmund mechanism for the sputtering process (Murty et al., 1998a; Strobel et al., 2001). Unlike these other simulations, our model considers both the Sigmund mechanism and thermally activated diffusion of surface defects satisfying detail balance.

A brief description of the concept behind the KMC simulation is discussed below; a fuller description can be found in Chason et al. (2006). The positions of all the atoms on a surface are assigned to an element in a two-dimensional lattice (known as a solid-on-solid model). A schematic representation of different surface processes considered in the KMC is shown schematically in Figure 4. Note that we also allow the motion of vacancies in the surface to occur by the hopping of atoms adjacent to it. This is important because we believe that mobile vacancy defects play a significant role in surface evolution during ion sputtering.

All the transitions that can occur on the surface are assigned a rate based on the local configuration. The rate of transition between two sites i and j is based on a thermally activated process in which the barrier to the transition ($E_{i,j}$) is

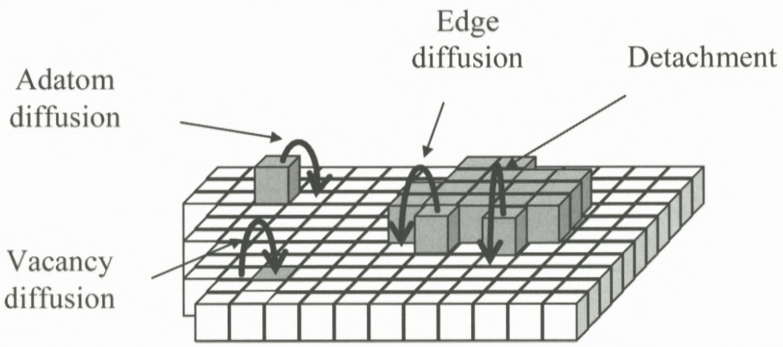

Figure 4. Schematic of surface transport processes considered in the kinetic Monte Carlo simulation of sputtering. Each surface process has an activation energy and transition rate associated with it. Note that in the simulation vacancy diffusion is allowed to occur at a rate equal to adatom diffusion.

equal to an activation energy (E_a) plus the difference in bond energy between the two configurations. The change in bond energy between two configurations is determined by counting the change in the number of nearest neighbors ($n_i - n_j$) and multiplying by a constant energy per bond (E_{bond}) if the number of bonds decreases. The rate of a transition is therefore

$$R_{i,j} = \omega \, \mathrm{e}^{-E_{i,j}/kT}, \tag{8}$$

where $E_{i,j} = E_a$ if the number of bonds does not decrease ($n_i \leq n_j$) or $E_{i,j} = E_a + (n_i - n_j)E_{\text{bond}}$ if the number of bonds decreases ($n_i > n_j$). The attempt frequency ω is a constant that is taken as 10^{12} s^{-1} in the current work. Keeping track of bond energy in this way ensures that detailed balance is preserved, i.e., the rate of a transition between two sites in the forward and backward direction is properly related to the difference in energy between the sites.

Lists of all the surface positions at which atomic transitions can occur and their associated transition rates are maintained in the computer simulation as the surface evolves. Events are chosen from these lists randomly with a probability that is proportional to the transition rate. In this way, atomic level events are performed on the surface at a rate that is on average proportional to the transition rate for that process.

The process described above is able to simulate the evolution of the surface due to diffusive processes. The removal of atoms from the surface via sputtering requires an additional mechanism. We use the same Sigmund mechanism utilized in the continuum approach to model the sputtering process in the KMC simulations. For an individual incident ion trajectory, the position at which it strikes the surface is chosen randomly and the energy deposition at all the points on the surface is

Table 1. List of parameters used in the kinetic Monte Carlo simulations.

Activation energy (E_a)	0.8 eV Note: a value of 1.0 eV was used for diffusion along the edge of a step.
Bond energy (E_{bond})	0.2 eV
Temperature (T)	187–250°C
Flux (f)	0.15–6.0 monolayers/s
Ion parameters:	
θ	45 deg
a	20
$\sigma = \mu$	10
Y	2 atoms/ion

then calculated using Equation (1). Unlike the continuum approach, the surface height is not reduced incrementally at each point based on the calculated energy deposition. Instead the energy deposition is used to determine the probability of sputtering from each site on the surface; the Monte Carlo algorithm is then used to choose which site to perform the sputtering event based on the relative probabilities.

4. Results of KMC Simulations and Comparison with Continuum Theory

We performed KMC simulations of surface evolution during sputtering under a range of processing conditions in order to study the dependence of the ripple growth rate and wavelength on the processing conditions. The parameters used in the simulation are given in Table 1. The results described here have been presented more fully in Chason et al. (2006) but are reviewed here in order to provide a comparison between the simulations and the continuum theory.

The morphology of ripples produced by the KMC program under different simulation conditions is shown in Figure 5. Figure 5a corresponds to simulated sputtering at $f = 1$ monolayer/s, $T = 187$°C and a fluence of 45 monolayers and Figure 5b corresponds to $f = 1$ monolayer/s, $T = 250$°C and a fluence of 70 monolayers. The time evolution of the simulated ripple amplitude and wavelength for the same conditions is shown in Figure 6. Aside from an initial transient, the wavelength of the ripples remains fairly constant over the entire range of the sim-

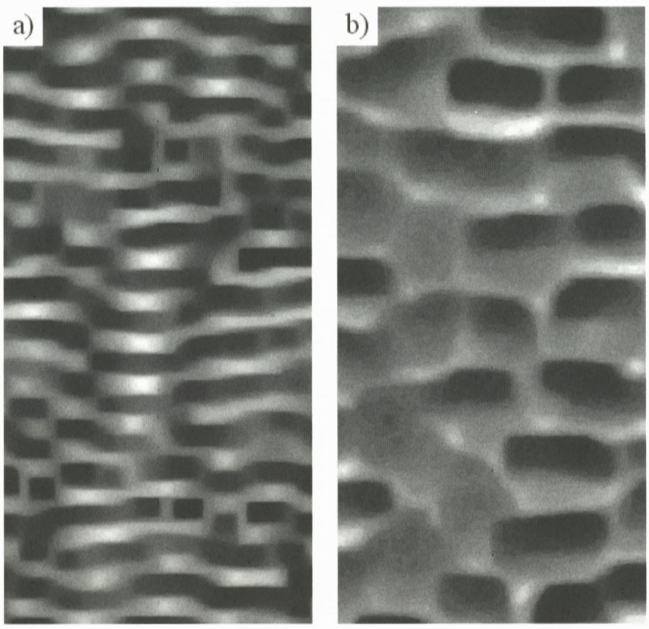

Figure 5. Surface morphology produced by KMC simulation with (a) $T = 187°C$, fluence = 45 monolayers and (b) $T = 250°C$, fluence = 70 monolayers. The flux for both cases is 1 monolayer/s.

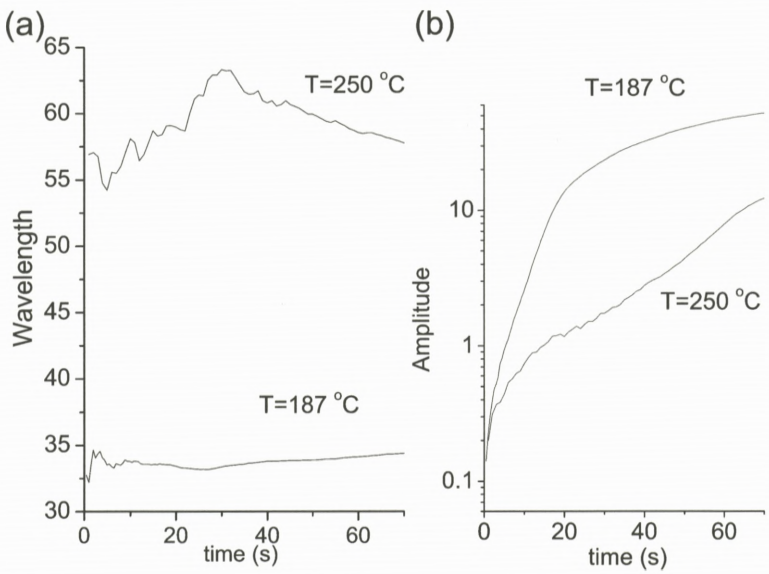

Figure 6. Evolution of (a) wavelength and (b) amplitude of the ripples produced by the KMC simulations. Temperature for the simulation is indicated on the figure.

ulation. The amplitude increases exponential in the early stages, though saturation is reached for larger amplitudes. Both of these features, a fixed wavelength and an exponential growth in the early stages are consistent with the expected behavior from the instability model. The amplitude saturation can also be addressed by including higher order non-linear terms (Cuerno and Barabasi, 1995; Park et al., 1999) in the continuum theory, but we have restricted our analysis of the KMC studies to the linear regime where amplitudes are small and the approximations of the Sigmund model are most valid.

Surface defects (adatoms and vacancies) play a major role in determining smoothing processes on the surface (Erlebacher et al., 1999; Chan and Chason, 2005). Unlike experiments, in the KMC simulation we can monitor the concentration of defects on the surface directly during the surface morphology evolution. The primary defect that we observe on the surface is the vacancy, which is consistent with the fact that we directly produce vacancies in the simulation when atoms are removed from surface sites by sputtering. The concentration of defects across the surface appears to be uniform and is not correlated with the surface morphology. The defect concentration depends on both the temperature and the ion flux with the concentration increasing with increasing ion flux and decreasing with increasing temperature. Fitting the temperature and flux dependence to a power law behavior gives good agreement over the entire range of the simulation conditions using the form $(f/D)^{0.48}$.

By performing simulations under different conditions, we have also studied the flux and temperature dependence of the ripple wavelength. The temperature dependence of the simulated ripple wavelength (shown in Figure 7) can be compared directly with the continuum theory using Equation (7b). Using the fact that $v_{\max}$ and $B_{I,\max}$ depend only on the flux and not on temperature, the continuum theory predicts that the wavelength should depend on the following parameteric form:

$$\lambda^*(T, f) = \frac{2\pi}{k^*} \propto \sqrt{\frac{D_s C}{fT} + A_I}, \tag{9}$$

where A_I is a constant independent of flux or temperature. In evaluating this expression, we can use the measured value of the defect concentration for each temperature and flux. The only unknown parameters required to compare this form with the data are A_I, an overall normalization constant and the activation energy for the diffusivity. The fit to this form is shown as the solid line in Figure 7. The value for the activation energy determined from the fit is 0.86 eV, in good agree with the value of 0.8 used as an input in the simulation.

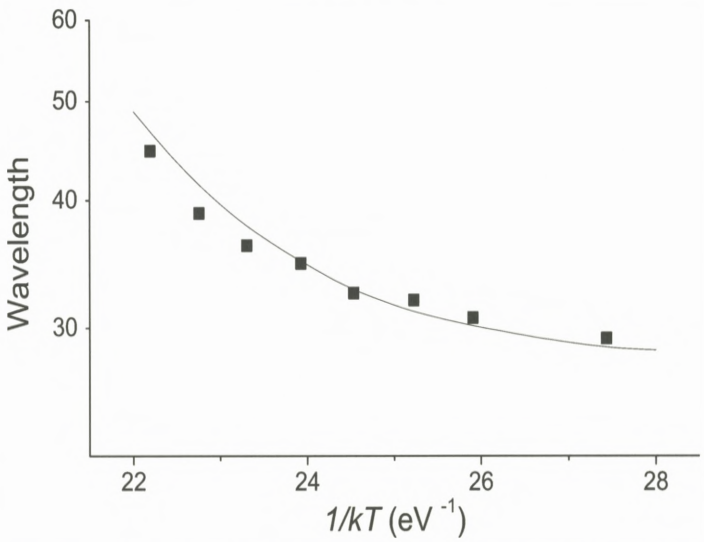

Figure 7. Dependence of simulated ripple wavelength on temperature. The solid line represents least squares fit to analytical form described in text.

5. Conclusion

The morphological evolution produced by the KMC simulation shows that the Sigmund theory captures the essential physics required to produce Bradley–Harper type ripples in the early stages of sputtering. Furthermore, comparison of the continuum theory with the KMC results indicates that the analytical theory does a good job of capturing the balance between roughening by sputter removal and smoothing by surface diffusion, e.g., the continuum equations quantitatively account for the temperature dependence of the wavelength of ripples produced by the simulation. The agreement is somewhat surprising since the diffusional smoothing used in the continuum model is not appropriate for the crystalline, stepped surface used in the simulation. In spite of this, it provides good agreement over a wide range of parameters studied. It is worth noting that non-linear effects such as amplitude saturation are observed in the simulation, even though we have restricted our analysis to the linear instability regime. These effects can incorporated into the continuum analysis by using higher-order non-linear terms but we have not considered them here.

Although the simulations agree well with the continuum theory, this does not mean that the Bradley–Harper theory is a complete description for early-stage ripple formation in experimental systems. Measurements of the rate of ripple

formation on Cu (Chan et al., 2004a), Ge (Chason et al., 1994) and Si (Brown and Erlebacher, 2005) surfaces are significantly lower than predicted by the theory. This suggests that there may be other roughening mechanisms in experimental systems beyond the Sigmund that have not been included in the simulations or the continuum model.

Furthermore, over a wider range of parameters than those discussed here, transitions to other type of roughening behavior can be observed both in the experiments and the simulations. These studies are discussed in other references (Chan and Chason, 2006; Chason and Chan, 2006).

Acknowledgements

This work has benefited greatly from collaboration and helpful discussions with many others including Vivek Shenoy, Jonah Erlebacher, Michael Aziz, Ashwin Ramasubramanian and M.S. Bharathi. The authors also gratefully acknowledge the support of the US Department of Energy under contract DE-FG02-01ER45913 and EC acknowledges the National Science Foundation under contract CMS-0210095.

References

Bradley R.M. and Harper J.M.E. (1988): Theory of ripple topography induced by ion Bombardment. J Vac Sci Technol A **6**, 2390–2395

Brown A.-D. and Erlebacher J. (2005): Temperature and fluence effects on the evolution of regular surface morphologies on ion-sputtered Si(111). Phys Rev B **72**, 075350

Carter G. (2001): The physics and applications of ion beam erosion. J Phys D: Appl Phys **34**, R1–R22

Carter G. and Vishnyakov V. (1996): Roughening and ripple instabilities on ion-bombarded Si. Phys Rev B **54**, 17647–17653

Chan W.L. and Chason E. (2005): Sputter ripples and radiation-enhanced surface kinetics on Cu(001). Phys Rev B **72**, 165418

Chan W.L. and Chason E. (2006): Morphology of ion sputtered Cu(001) surface: Transition from unidirectional roughening to bidirectional roughening. Nucl Instrum Methods B **242**, 228–231

Chan W.L., Pavenayotin N. and Chason E. (2004a): Kinetics of ion-induced ripple formation on Cu(001) surface. Phys Rev B **69**, 245413

Chan W.L., Ramasubramaniam A., Shenoy V.B. and Chason E. (2004b): Relaxation kinetics of nano-ripples on Cu(001) surface. Phys Rev B **70**, 245403

Chason E. and Chan W.L. (2006): Kinetics mechanisms in ion-induced ripple formation on Cu(001) surfaces. Nucl Instrum Methods B **242**, 232–236

Chason E. and Dodson B.W. (1991): Effect of step edge transition rates and anisotropy in simulations of epitaxial-growth. J Vac Sci Technol A **9**, 1545–1550

Chason E., Mayer T.M., Kellerman B.K., McIlroy D.T. and Howard A.J. (1994): Roughening instability and evolution of Ge(001) surface during ion sputtering. Phys Rev Lett **72**, 3040–3043

Chason E., Chan W.L. and Bharathi M.S. (2006): Kinetic Monte Carlo simulations of ion-induced ripple formation. Submitted

Cirlin E.-H. (1992): Auger electron spectroscopy and secondary ion mass spectrometry depth profiling with sample rotation. Thin Solid films **220**, 197–203

Costantini G., Rusponi S., de Mongeot F.B., Boragno C. and Valbusa U. (2001): Periodic structures induced by normal-incidence sputtering on Ag(110) and Ag(001): Flux and temperature dependence. J Phys: Condens Matter **13**, 5875–5891

Cuerno R. and Barabasi A.L. (1995): Dynamic scaling of ion-sputtered surfaces. Phys Rev Lett **74**, 4746–4749

Cuerno R., Makse H.A., Tomassone S., Harrington S.T. and Stanley H.E. (1995): Evolution from ripple morphology to rough morphology. Phys Rev Lett **75**, 4464–4467

Erlebacher J., Aziz M.J., Chason E., Sinclair M.B. and Floro J.A. (1999): Spontaneous pattern forming on ion bombarded Si(001). Phys Rev Lett **82**, 2330–2333

Erlebacher J., Aziz M.J., Chason E., Sinclair M.B. and Floro J.A. (2000): Nonclassical smoothening of nanoscale surface corrugations. Phys Rev Lett **84**, 5800–5803

Ernst H.-J. (1997): The pattern formation during ion bombardment of Cu(001) investigated with helium atom beam scattering. Surf Sci **383**, L755–L759

Facsko S., Dekorsy T., Koerdt C., Trappe C., Kurz H., Vogt A. and Hartnagel H.L. (1999): Formation of ordered nanoscale semiconductor dots by ion sputtering. Science **285**, 1551–1553

Frost F., Ziberi B., Höche T. and Rauschenbach B. (2004): The shape and ordering of self-organized nanostructures by ion sputtering. Nucl Instrum Methods B **216**, 9–19

Gago R., Vazquez L., Cuerno R., Varela M., Ballesteros C. and Albella J.M. (2001): Production of ordered silicon nanocrystals by low-energy ion sputtering. Appl Phys Lett **78**, 3316–3318

Habenicht S. (2001): Morphology of graphite surfaces after ion-beam erosion. Phys Rev B **63**, 125419

Hartmann A.K., Kree R., Geyer U. and Kölbel M. (2002): Long-term effect in a simulation model of sputter erosion. Phys Rev B **65**, 193403

Herring C. (1950): Effect of change of scale on sintering phenomena. J Appl Phys **21**, 301–303

Israeli N. and Kandel D. (2000): Decay of one-dimensional surface modulations. Phys Rev B **62**, 13707–13717

Jeong H.-C. and Williams E.D. (1999): Steps on surfaces: Experiment and theory. Surf Sci Rep **34**, 175–294

Kalff M., Comsa G. and Michely T. (2001): Temperature dependent morphological evolution of Pt(111) by ion erosion: destabilization, phase coexistence and coarsening. Surf Sci **486**, 103–135

Koponen I., Hautala M. and Sievanen O.-P. (1997): Simulations of ripple formation on ion-bombarded solid surfaces. Phys Rev Lett **78**, 2612–2615

Makeev M.A. and Barabasi A.-L. (1997): Ion-induced effective surface diffusionin ion sputtering. Appl Phys Lett **71**, 2800–2802

Makeev, M.A., Cuerno R. and Barabasi A.L. (2002): Morphology of ion-sputtered surfaces. Nucl Instrum Methods B **197**, 185–227

Malis O., Brock J.D., Headrick R.L., Yi M.-S. and Pomeroy J.M. (2002): Ion-induced pattern formation on Co surfaces: An x-ray scattering and kinetic Monte Carlo study. Phys Rev B **66**, 035408

Margetis D., Aziz M.J. and Stone H.A. (2004): Continuum description of profile scaling in nanostructure decay. Phys Rev B **69**, 041404

Mayer T.M., Chason E. and Howard A. (1994): Roughening instability and ion induced viscous relaxation of SiO_2 surfaces. J Appl Phys **76**, 1633–1643

Michely T., Kalff M., Comsa G., Strobel M. and Heinig K.H. (2001): Step edge diffusion and step atom detachment in surface evolution: Ion-erosion of Pt(111). Phys Rev Lett **86**, 2589–2592

Mullins W.W. (1959): Flattening of a nearly plane solid surface due to capillarity. J Appl Phys **30**, 77–83

Murty M.V.R., Cowles B. and Cooper B.H. (1998a): Surface smoothing during sputtering: Mobile vacancies versus adatom detachment and diffusion. Surf Sci **415**, 328–335

Murty M.V.R., Curcic T., Judy A., Cooper B.H., Woll A.B., Brock J.D., Kycia S. and Headrick R.L. (1998b): X-ray scattering study of the surface morphology of Au(111) during Ar^+ ion irradiation. Phys Rev Lett **80**, 4713–4716

Park S., Kahng B., Jeong H. and Barabasi A.-L. (1999): Dynamics of ripple formation in sputter erosion: Nonlinear phenomena. Phys Rev Lett **83**, 3486

Pedemonte L., Bracco G., Boragno C., de Mongeot F.B. and Valbusa U. (2003): Smoothing of nanoscale surface ripples studied by He atom scattering. Phys Rev B **68**, 115431

Politi P. and Villain J. (1996): Ehrlich-Schwoebel instability in molecular beam epitaxy: A minimal model. Phys Rev B **54**, 5114–5129

Ritter M., Stindtmann M., Farle M. and Baberschke K. (1996): Nanostructuring of the Cu(001) surface by ion bombardment: A STM study. Surf Sci **348**, 243–252

Rusponi S., Costantini G., Boragno C. and Valbusa U. (1998): Scaling laws of the ripple morphology on Cu(110). Phys Rev Lett **81**, 4184–4187

Shenoy V.B., Ramasubramaniam A. and Freund L.B. (2003): A variational approach to nonlinear dynamics of nanoscale surface modulations. Surf Sci **529**, 365–383

Shenoy V.B., Ramasubramaniam A., Ramanarayan H., Tambe D.T., Chan W.-L. and Chason E. (2004): Influence of step-edge barriers on the morphological relaxation of nanoscale ripples on crystal surfaces. Phys Rev Lett **92**, 256101

Sigmund P. (1969): Theory of sputtering I. Sputtering yield of amorphous and polycrystalline targets. Phys Rev **184**, 383–416

Sigmund P. (1973): A mechanism of surface microroughening by ion bombardment. J Mater Sci **8**, 1545–1553

Stepanova M. and Dew S.K. (2004): Surface relaxation in ion-etch nanopatterning. Appl Phys Lett **84**, 1374–1376

Stevie F.A., Kahora P.M., Simons D.S. and Chi P. (1988): Secondary ion yield changes in Si and GaAs due to topography changes during O_2^+ or Cs^+ ion bombardment. J Vac Sci Technol A **6**, 76–80

Strobel M., Heinig K.H. and Michely T. (2001): Mechanisms of pit coarsening in ion erosion of fcc(111) surfaces: A kinetic 3D lattice Monte-Carlo study. Surf Sci **486**, 136–156

Umbach C.C., Headrick R.L. and Chang K.-C. (2001): Spontaneous nanoscale corrugation of ion-eroded SiO_2: The role of ion-irradiation-enhanced viscous flow. Phys Rev Lett **87**, 246104

Valbusa U., Borangno C. and de Mongeot F.B. (2002): Nanostructuring surfaces by ion sputtering. J Phys: Condens Matter **14**, 8153–8175

Villain J. (1991): Continuum model of crystal – Growth from atomic-beams with and without desorption. J Phys (Paris) **1**, 19–42

Wittmaack K. (1998): Artifacts in low-energy depth profiling using oxygen primary ion beams: Dependence on impact angle and oxygen flooding conditions. J Vac Sci Technol B **16**, 2776–2785

Yewande E.O., Hartmann A.K. and Kree R. (2005): Propagation of ripples in Monte Carlo models of sputter-induced surface morphology. Phys Rev B **71**, 195405

Ziegler J.F. and Biersack J.P. (2000): SRIM-2000.40, IBM Co., Yorktown, NY